Heterometallic Nanostructures

DOI: 10.1002/anie.201007755

Plasmon-Mediated Synthesis of Heterometallic Nanorods and Icosahedra**

*Mark R. Langille, Jian Zhang, and Chad A. Mirkin**

The controlled synthesis of heterometallic nanocrystals is highly desirable because of the unique optical, electronic, magnetic, and catalytic properties imparted by each component,[1–7] as well as new features that can arise from the effective coupling of different materials.[8–10] The realization of both positional and morphological control over each component within these structures will provide even greater tunability of their resulting properties. One synthetic approach to generate such nanostructures is to use a seed-mediated strategy where a secondary metal is epitaxially deposited onto seed particles that have similar lattice parameters.[11–13] Recently, we showed that certain noble metals can be used both as seed particles and electron microscopy labels to follow heterometallic particle growth and shape evolution processes.[11] Indeed, by utilizing this strategy, one can prepare and study the growth of heterometallic core–shell nanostructures such as triangular prisms,[11,14] cubes,[12,15] octahedra,[12] rods,[16] and plates.[13] However, achieving precise shape control of heterometallic nanostructures is still synthetically challenging.

Plasmon-mediated syntheses of metallic nanostructures are often high-yielding and provide outstanding shape control in the context of prisms,[17–19] bipyramids,[20,21] decahedra,[22,23] and tetrahedra.[24] We first introduced the concept of plasmonic seed-mediated synthesis with the discovery that small spherical Ag nanoparticles could be irradiated with light of appropriate wavelengths to be selectively converted into triangular nanoprisms.[17,18] Mechanistic studies of this reaction have shown that the reduction of Ag^+ ions by trisodium citrate is catalyzed by Ag nanoparticles under plasmon excitation to form small nanoprisms.[25,26] The nanoprisms continue to grow until their surface plasmon resonance (SPR) is red-shifted from the excitation wavelength, allowing precise control over their edge length. Such facile photomediated size control has also been demonstrated for the synthesis of highly monodisperse Ag right-triangular bipyramids.[20] Furthermore, we have shown that, in conjunction with a seeded-synthesis technique, this plasmon-mediated method can be used to synthesize bimetallic triangular core–shell nanoprisms from spherical and prismatic gold seeds by adjusting the excitation wavelength to the SPR of the plasmonic seed.[11] However, the resulting bimetallic core–shell structures generated from this plasmonic seed-mediated approach are triangular prisms, regardless of the shape of the seed particles (spheres or prismatic plates).

Herein, we describe a plasmon-mediated approach to the synthesis of shape-controlled heterometallic nanostructures. By simply adjusting the pH value of the solution, the light-induced overgrowth of Ag onto well-defined penta-twinned Au decahedra nanoparticle seeds can be controlled to yield either heterometallic nanorods or icosahedra (Figure 1). We demonstrate that the pH value affects the reduction rate of

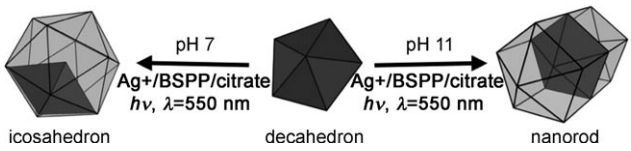

Figure 1. pH-dependent plasmon-mediated growth processes involving the photodeposition of Ag on plasmonic decahedral Au seeds. Au dark gray; Ag light gray.

Ag^+ ions, which affects the growth kinetics and leads to the different morphologies of the heterometallic structures. To the best of our knowledge, this is the first report of the realization of heterometallic icosahedral nanostructures from decahedral core particles.

Au decahedra with an average edge length of 40 nm (Figure 2 A) were prepared (shape yield ≈ 70 %) according to reported procedures[27] and used as plasmonic seeds to control the nucleation and growth of Ag shells and act as electron microscopy labels to monitor particle growth. In a typical synthesis of Au–Ag heterometallic nanorods, an aqueous solution of $AgNO_3$, sodium citrate, bis(*p*-sulfonatophenyl)-phenylphosphine dihydrate potassium salt (BSPP), and Au decahedra was prepared, and the pH of the reaction solution was raised to 11 by the addition of 0.1 M NaOH (see the Experimental Section). This solution was then irradiated for 8 h with a 150 W halogen lamp using a bandpass filter centered at 550 ± 20 nm, which is close to the maximum absorbance of the Au decahedra at 580 nm (Figure S1 in the Supporting Information). The solution turned pink after

[*] M. R. Langille,[+] J. Zhang,[+] Prof. C. A. Mirkin
Department of Chemistry and
International Institute of Nanotechnology
Northwestern University
2145 Sheridan Road, Evanston, IL 60208-3113 (USA)
Fax: (+1) 847-467-5123
E-mail: chadnano@northwestern.edu

[+] These authors contributed equally to this work.

[**] This work was supported by the MRSEC program of the National Science Foundation at the Material Research Center of Northwestern University. The electron microscopy work was performed in the EPIC facilities of NUANCE Center at Northwestern University. NUANCE Center is supported by NSF-NSEC, NSF-MRSEC, Keck Foundation, the State of Illinois, and Northwestern University. C.A.M. is grateful for an NSSEF Fellowship from the DoD.

Supporting information for this article is available on the WWW under http://dx.doi.org/10.1002/anie.201007755.

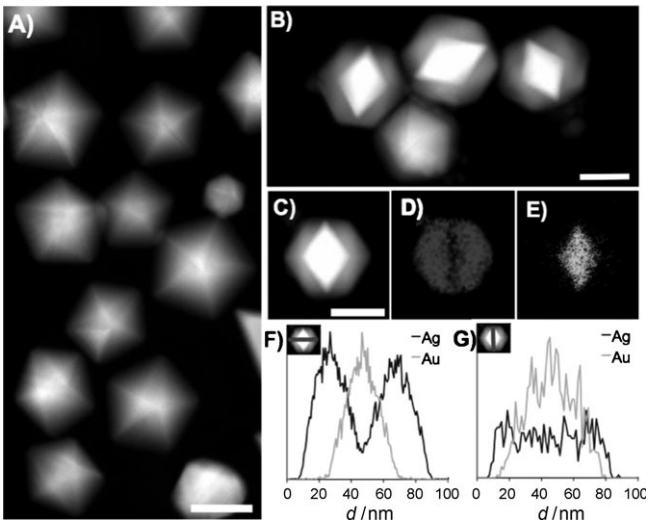

Figure 2. A) Representative STEM image of the Au decahedral cores. B) Group of heterometallic nanorods. C) Individual heterometallic nanorod. EDS data from the particle in (C) showing D) the Ag shell and E) the Au core. The distribution of Ag and Au components is shown along cross-sections that run F) parallel and G) perpendicular to the pentagonal axis of the decahedron. Scale bars: 50 nm; d = distance.

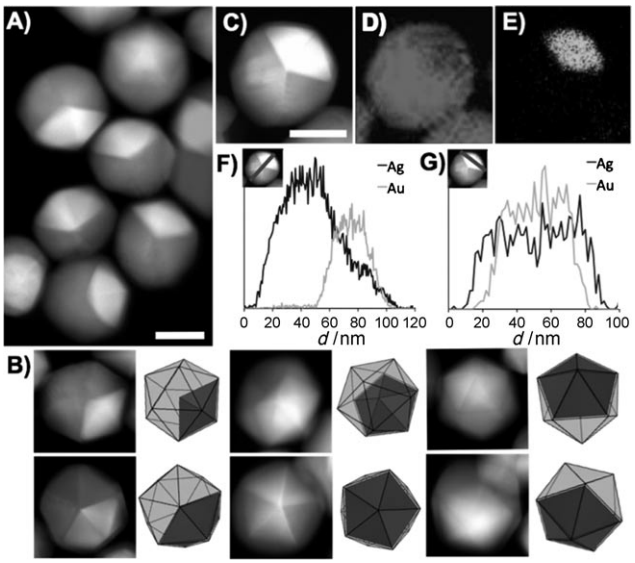

Figure 3. A) Representative STEM image of the heterometallic icosahedra. B) Images of individual heterometallic icosahedra in various orientations next to their corresponding CAD model in the identical orientation. C) Individual heterometallic icosahedron. EDS data from the particle in (C) showing D) the Ag shell and E) the Au core. The distribution of Ag and Au components are shown for cross-sections that run along (F) and G) perpendicular to the pentagonal axis of the decahedron. Scale bars: 50 nm; d = distance.

10 min of irradiation and became opaque orange after 1 h. There was no change in color with further irradiation, even for an additional 24 h, which was the longest time period studied.

These nanostructures can be identified as heterometallic penta-twinned nanorods from scanning transmission electron microscopy (STEM) images (Figure 2B). When the nanorods are viewed lying down on the TEM grid, the Au decahedral cores have a diamond-shaped projection with brighter contrast than the Ag shells; this difference arises from electron-scattering differences between the Au and Ag components. The Au–Ag core–shell heterometallic nanorods were also characterized by energy dispersive X-ray spectroscopy (EDS; Figure 2C–G). The distributions of the Au and Ag components along and perpendicular to the pentagonal axes are shown in Figure 2F and 2G, respectively. The EDS data indicate that the nanostructures have distinct core and shell components. Ag is deposited selectively along the pentagonal axes of the decahedra, and there is no Au/Ag alloy in the heterometallic nanorod structures. The distribution of Au and Ag along the cross-sections suggests that the entire surface of the Au decahedra is coated with Ag. The Ag shell extends beyond the Au cores in all directions, but only by a few nanometers along the direction perpendicular to the pentagonal axes (Figure 2G).

The pH value is an important factor in the plasmon-mediated synthesis of Ag nanostructures.[19] We have previously demonstrated that pH can inhibit the bimodal growth behavior for Ag triangular nanoprisms, thus allowing the synthesis of nanoprisms with uniform and tailorable dimensions.[19] In the present study, we show that the growth of Ag on Au decahedra can also be controlled by pH, but with significantly different resulting morphologies. Indeed, by simply switching the pH value of the reaction solution from 11 (for the preparation of nanorods) to 7, bimetallic icosahedra that contain identifiable gold seeds are formed (Figure 3A). In this case, as the growth solution containing the decahedra seeds was irradiated, the color changed from light purple to pink after 30 min and then became faint pink after 5 h, without any noticeable changes upon further irradiation. The structures of the heterometallic icosahedra were extensively studied by STEM and compared to a computer-aided-design (CAD) model (Figure 3B). Both the shape and contrast of the particles correlate well with the STEM images and CAD model, confirming the heterometallic icosahedral morphology.

The icosahedra were also characterized by EDS (Figure 3C–G). Elemental maps indicate that a single Au decahedron is asymmetrically located in each icosahedron, and EDS line profiles of cross-sections along the pentagonal axes of each decahedron confirm that the gold seed is asymmetrically positioned (Figure 3F). Ag is deposited over the entire surface of the Au decahedron, and the Au is not exposed. This observation is supported by the data obtained from EDS line scans along cross-sections perpendicular to the pentagonal axes of the decahedron, where it shows that the distribution of the Ag components extends beyond the distribution of the Au components (Figure 3G).

Heterometallic icosahedra nanoparticles with an asymmetric metallic distribution can be produced using this plasmon-mediated synthetic method. While the symmetric overgrowth of Ag onto Au decahedra to produce Au–Ag heterometallic nanorods can be achieved by using either the method presented in this study or by using a recently reported polyol synthesis,[16] the asymmetric overgrowth of Ag on such

nanoparticle seeds has not been described. In crystallography, multiply twinned decahedra and icosahedra are related structures. A decahedron can be considered to be the assembly of 5 single-crystalline tetrahedral units joined together by (111) twin planes with a common axis along the [110] direction, and consequently has 10 (111) facets exposed on its surface. On the other hand, an icosahedron is geometrically composed of 20 tetrahedral units.[28,29] For the construction of the heterometallic icosahedron, an Au decahedron provides 5 tetrahedral units, while the remaining 15 tetrahedral units are composed of Ag.

To better understand the transformation from a decahedron to an icosahedron, we used STEM to characterize several intermediate particles in the icosahedra reaction in order to determine the growth process, which is illustrated in Figure 4. We propose that this asymmetric transformation

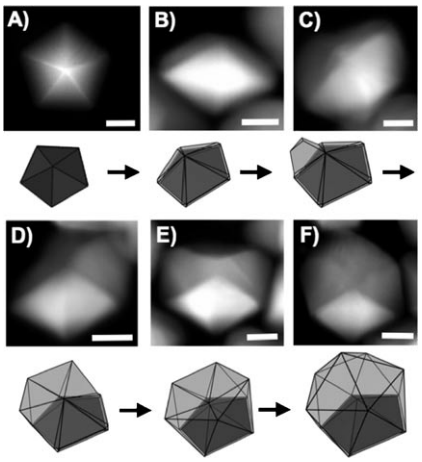

Figure 4. STEM images and CAD models illustrating the growth of an Au decahedron to an Au–Ag heterometallic icosahedron. Scale bars: 25 nm.

occurs by the successive twinning and growth of tetrahedral units from the decahedral cores. Ag is first deposited isotropically over the entire surface of the Au decahedron followed by the anisotropic deposition of Ag onto one side of the decahedron (Figure 4B). The formation of an icosahedron is initiated by the development of a twin plane on one of the (111) faces of the decahedron and the subsequent growth of a Ag tetrahedral unit. At this stage, a single Ag tetrahedron can be observed on top of the decahedral core (Figure 4C). The newly exposed faces of the Ag tetrahedral unit provide additional (111) surfaces for subsequent twin-plane formation, thus promoting the growth of adjoining tetrahedral units (Figure 4D). Note that the presence of twin planes is assumed based on previous reports regarding the twin structures of decahedra and icosahedra.[28,29] Eventually, by successive twinning and growth events, Ag asymmetrically grows outwards over the entire surface of the Au decahedron, yet there remains a decahedron-shaped indentation opposite the Au decahedral core (Figure 4E). In the final stage of growth, Ag is deposited into this indentation until the final heterometallic icosahedron morphology is obtained (Figure 4F). The step-by-step, successive growth of multiply twinned nanostructures is consistent with previous observations in other systems.[28,30] However, by utilizing plasmon-mediated methods, we demonstrate that it is possible to achieve the shape transformation from an Au decahedron to an Au–Ag heterometallic icosahedron.

Reaction kinetics can significantly affect the growth of metal nanoparticles[31] and, for that reason, we wanted to determine if the different heterometallic nanoparticle morphologies observed at the two pH values could be attributed to differences in reaction rates. The chemical reaction for the plasmon-mediated reduction of Ag^+ by sodium citrate has been proposed in previous work.[25,26] Briefly, seed particles under plasmon excitation catalyze the reduction of Ag^+ to Ag^0 and the oxidation of citrate ions to 1,3-acetonedicarboxylate and carbon dioxide (Scheme 1). The dependence of the

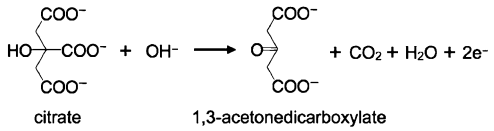

Scheme 1. Proposed oxidation half-reaction for the plasmon-mediated reduction of Ag^+ ions.[25,26]

oxidation half-reaction on hydroxide ion concentration allows for the reaction rate to be controlled by pH.[21] Indeed, by monitoring the concentration of Ag^+ ions using inductively coupled plasma atomic emission spectroscopy (ICP-AES) over the course of the reactions, we found that the Ag^+ concentration decreases more rapidly for the reaction at pH 11 than at pH 7, and is consistent with the faster color changes observed for the reaction carried out at a higher pH value (Figure 5). The concentration of Ag^+ ions at either pH value does not reach zero because the BSPP ligand binds to aqueous Ag^+,[32,33] thereby inhibiting the complete reduction of all of the Ag^+ ions in solution. Additionally, the final Ag^+ concentration is higher at pH 7 than pH 11 because of the lower reducing ability of citrate at lower pH values.[34]

The observation of two different heterometallic nanoparticle morphologies can be partially explained by the pH-dependent reaction rates. In the fast reaction at pH 11, Ag is

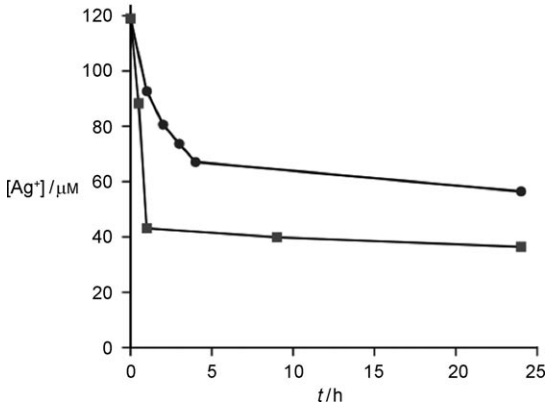

Figure 5. ICP-AES data monitoring the concentration of Ag^+ for the plasmon-mediated reactions that generate icosahedra at pH 7 (●) and nanorods at pH 11 (■).

deposited onto the (111) faces of the Au decahedral core particles with crystal growth occurring along the [110] direction to generate a rod morphology with exposed (100) side facets and (111) end facets.[31] A similar deposition preference has been observed in our recent study of the plasmon-meditated growth pathway for Ag bipyramids at high pH values, where the preferential deposition on the (111) facets of the planar-twinned seeds results in the formation of (100)-faceted Ag right-triangular bipyramids.[21]

On the other hand, the slower reaction at pH 7 generates icosahedra that are bound entirely by (111) facets. This result is also consistent with previous observations that the slower reaction conditions yield (111)-faceted nanoprisms.[21] However, the question remains as to why we observe asymmetric growth into icosahedra rather than epitaxial growth of decahedra, which would also be bound by low-energy (111) facets. Generally, the transformation from a decahedron to an icosahedron requires the development of new twin planes whereas the epitaxial overgrowth of a decahedron requires the continued propagation of pre-existing twin planes.[28] Both processes have been previously observed in studies of Au[35,36] and Ag[30,36] nanocrystals, and have been shown to occur in molecular-dynamics simulations.[37] Although the driving force is not well understood, theoretical calculations have shown that the deposition rate can affect the growth pathway.[38] In this study, we found that by incrementally adding small amounts of Ag^+ ions rather than adding all of the Ag^+ at the beginning of the reaction, effectively reducing the reaction rate, we were able to achieve the epitaxial growth of Ag decahedral shells at pH 7 (Figure S2). The extremely slow reduction of a small amount of Ag^+ allows one to achieve epitaxial growth on the Au decahedral cores, leading us to believe that it is the relatively high initial concentration of Ag^+ that leads to the formation of twin planes and consequently, the growth of icosahedral heterometallic nanocrystals. A detailed investigation of the mechanism and driving force for the observed twinning and growth of heterometallic icosahedra from decahedral cores is currently underway.

In conclusion, we have demonstrated a pH-controlled, plasmon-mediated synthesis of heterometallic nanorods and icosahedra. The reduction rate of Ag^+ ions is controlled by pH, thereby allowing Ag to be deposited onto Au decahedral cores either epitaxially, to generate (100)-faceted nanorods at high pH values, or non-epitaxially, to form twin planes and ultimately generate (111)-faceted icosahedra at low pH values. The unique transformation from a decahedron to an icosahedron occurs by the development of tetrahedral units through successive twinning, thus demonstrating that asymmetric growth can be achieved for core–shell heterometallic nanostructures. This process proves to be an advance for both heterometallic nanocrystal synthesis and plasmon-mediated synthetic methods. Note that the yields that result from this synthetic method are very sensitive to the quality of the Au plasmonic seeds. Mechanistically, this observation indicates that the plasmon-mediated reduction of Ag^+ onto Au cores is dependent on both the shape and structural defects (e.g., twin planes, stacking faults) of the plasmonic seed. However, as synthetic methods improve and Au seeds of very high quality can be generated, this photomediated synthetic method has the potential to be a highly controllable procedure for generating heterometallic nanostructures. This technique, in principle, can be adapted to prepare nanoparticles with other core–shell morphologies by using different Au core structures, and this study is currently underway.

Experimental Section

Materials: Gold(III) chloride trihydrate (>99.9%), silver nitrate (99.998%), trisodium citrate dihydrate (99.9%), sodium hydroxide (99.99%), polyvinylpyrrolidone (PVP; M_W 55000), diethylene glycol (DEG; 99%), and ethanol (99.5%) were purchased from Aldrich and used as received. BSPP was purchased from Strem Chemicals, Inc. In all cases, water was purified with a Barnstead NANOpure water purification system (resistance = 18.1 MΩ).

Instrumentation: STEM imaging was performed on either a JEOL JEM-2100F TEM or a Hitachi HD-2300 STEM. All of the irradiation experiments were performed with a halogen lamp (Dolan-Jenner, MI-150) as the light source. An optical band-pass filter (25 mm diameter, Intor Inc.) centered at 550 ± 20 nm was employed to control the irradiation wavelength. ICP-AES experiments were performed on a Varian ICP-AES spectrometer.

Synthesis of Au decahedra: Previously reported procedures were followed for the synthesis of Au decahedra.[27] In brief, PVP (3.0 g, 27.0 mmol in terms of monomer) was dissolved in DEG (12.5 mL) and the mixture was heated to reflux for 5 min under rapid stirring. A solution of $HAuCl_4$ (10.0 mg, 0.025 mmol) in DEG (1.0 mL) was quickly injected and left to react for 10 min. The Au decahedra were diluted with ethanol (20 mL) and purified by centrifugation at 13.5 krpm for 30 min. The particles were washed three times with ethanol and then transferred into water. After additional washing with water, the particles were resuspended in water (6 mL). This procedure resulted in Au decahedra with an average edge length of 40 nm with a shape yield of approximately 70%.

Heterometallic nanorods and icosahedra: Heterometallic nanorods were synthesized by mixing NANOPure water (19.2 mL), $AgNO_3$ (0.25 mL, 10 mM), BSPP (0.25 mL, 10 mM), and sodium citrate (0.3 mL, 0.1M) in a 24 mL glass vial. NaOH (1 mL, 0.1M) was added to the mixture, followed by the Au decahedra (0.25 mL). The resulting solution was irradiated for 8 h with a 150 W halogen lamp coupled with an optical band pass filter centered at 550 ± 20 nm at an intensity of 0.4 W, measured by an optical power meter (Newport 1916-C) coupled with a thermopile detector (818P-010-12) with an active diameter of 12 mm. The distance between the lamp and the filter was maintained at 2 cm. For the synthesis of heterometallic icosahedra, all synthetic procedures were the same as the nanorod synthesis except that NaOH was not used.

Received: December 9, 2010
Published online: March 11, 2011

Keywords: gold · icosahedra · nanostructures · silver · surface plasmon resonance

[1] A. Wittstock, V. Zielasek, J. Biener, C. M. Friend, M. Bäumer, *Science* **2010**, *327*, 319–322.
[2] F. Tao, M. E. Grass, Y. Zhang, D. R. Butcher, J. R. Renzas, Z. Liu, J. Y. Chung, B. S. Mun, M. Salmeron, G. A. Somorjai, *Science* **2008**, *322*, 932–934.
[3] S. J. Hurst, E. K. Payne, L. Qin, C. A. Mirkin, *Angew. Chem.* **2006**, *118*, 2738–2759; *Angew. Chem. Int. Ed.* **2006**, *45*, 2672–2692.

[4] L. Qin, S. Park, L. Huang, C. A. Mirkin, *Science* **2005**, *309*, 113 – 115.
[5] L. Qin, M. J. Banholzer, X. Xu, L. Huang, C. A. Mirkin, *J. Am. Chem. Soc.* **2007**, *129*, 14870 – 14871.
[6] Y. W. Lee, M. Kim, Z. H. Kim, S. W. Han, *J. Am. Chem. Soc.* **2009**, *131*, 17036 – 17037.
[7] B. Lim, M. Jiang, P. H. C. Camargo, E. C. Cho, J. Tao, X. Lu, Y. Zhu, Y. Xia, *Science* **2009**, *324*, 1302 – 1305.
[8] J. Zhang, K. Sasaki, E. Sutter, R. R. Adzic, *Science* **2007**, *315*, 220 – 222.
[9] Z. Peng, H. Yang, *J. Am. Chem. Soc.* **2009**, *131*, 7542 – 7543.
[10] H. Lee, S. E. Habas, G. A. Somorjai, P. Yang, *J. Am. Chem. Soc.* **2008**, *130*, 5406 – 5407.
[11] C. Xue, J. E. Millstone, S. Li, C. A. Mirkin, *Angew. Chem.* **2007**, *119*, 8588 – 8591; *Angew. Chem. Int. Ed.* **2007**, *46*, 8436 – 8439.
[12] S. E. Habas, H. Lee, V. Radmilovic, G. A. Somorjai, P. Yang, *Nat. Mater.* **2007**, *6*, 692 – 697.
[13] B. Lim, J. Wang, P. H. C. Camargo, M. Jiang, M. J. Kim, Y. Xia, *Nano Lett.* **2008**, *8*, 2535 – 2540.
[14] H. Yoo, J. E. Millstone, S. Li, J.-W. Jang, W. Wei, J. Wu, G. C. Schatz, C. A. Mirkin, *Nano Lett.* **2009**, *9*, 3038 – 3041.
[15] F.-R. Fan, D.-Y. Liu, Y.-F. Wu, S. Duan, Z.-X. Xie, Z.-Y. Jiang, Z.-Q. Tian, *J. Am. Chem. Soc.* **2008**, *130*, 6949 – 6950.
[16] D. Seo, C. I. Yoo, J. Jung, H. Song, *J. Am. Chem. Soc.* **2008**, *130*, 2940 – 2941.
[17] R. Jin, Y. Cao, C. A. Mirkin, K. L. Kelly, G. C. Schatz, J. G. Zheng, *Science* **2001**, *294*, 1901 – 1903.
[18] R. Jin, Y. C. Cao, E. Hao, G. S. Métraux, G. C. Schatz, C. A. Mirkin, *Nature* **2003**, *425*, 487 – 490.
[19] C. Xue, C. A. Mirkin, *Angew. Chem.* **2007**, *119*, 2082 – 2084; *Angew. Chem. Int. Ed.* **2007**, *46*, 2036 – 2038.
[20] J. Zhang, S. Li, J. Wu, G. C. Schatz, C. A. Mirkin, *Angew. Chem.* **2009**, *121*, 7927 – 7931; *Angew. Chem. Int. Ed.* **2009**, *48*, 7787 – 7791.
[21] J. Zhang, M. R. Langille, C. A. Mirkin, *J. Am. Chem. Soc.* **2010**, *132*, 12502 – 12510.
[22] B. Pietrobon, V. Kitaev, *Chem. Mater.* **2008**, *20*, 5186 – 5190.
[23] X. Zheng, X. Zhao, D. Guo, B. Tang, S. Xu, B. Zhao, W. Xu, J. R. Lombardi, *Langmuir* **2009**, *25*, 3802 – 3807.
[24] J. Zhou, J. An, B. Tang, S. Xu, Y. Cao, B. Zhao, W. Xu, J. Chang, J. R. Lombardi, *Langmuir* **2008**, *24*, 10407 – 10413.
[25] C. Xue, G. S. Métraux, J. E. Millstone, C. A. Mirkin, *J. Am. Chem. Soc.* **2008**, *130*, 8337 – 8344.
[26] X. Wu, P. L. Redmond, H. Liu, Y. Chen, M. Steigerwald, L. Brus, *J. Am. Chem. Soc.* **2008**, *130*, 9500 – 9506.
[27] D. Seo, C. I. Yoo, I. S. Chung, S. M. Park, S. Ryu, H. Song, *J. Phys. Chem. C* **2008**, *112*, 2469 – 2475.
[28] H. Hofmeister, *Cryst. Res. Technol.* **1998**, *33*, 3 – 25.
[29] H. Hofmeister, *Z. Kristallogr.* **2009**, *224*, 528 – 538.
[30] M. Tsuji, M. Ogino, R. Matsuo, H. Kumagae, S. Hikino, T. Kim, S.-H. Yoon, *Cryst. Growth Des.* **2010**, *10*, 296 – 301.
[31] Y. Xia, Y. Xiong, B. Lim, S. E. Skrabalak, *Angew. Chem.* **2009**, *121*, 62 – 108; *Angew. Chem. Int. Ed.* **2009**, *48*, 60 – 103.
[32] S. Ahrland, J. Chatt, N. R. Davies, A. A. Williams, *J. Chem. Soc.* **1958**, 276 – 288.
[33] P. F. Barron, J. C. Dyason, P. C. Healy, L. M. Engelhardt, B. W. Skelton, A. H. White, *J. Chem. Soc. Dalton Trans.* **1986**, 1965 – 1970.
[34] K. C. Honeychurch, L. Gilbert, J. P. Hart, *Anal. Bioanal. Chem.* **2010**, *396*, 3103 – 3111.
[35] H. Hofmeister, *Thin Solid Films* **1984**, *116*, 151 – 162.
[36] K. Yagi, K. Takayanagi, K. Kobayashi, G. Honjo, *J. Cryst. Growth* **1975**, *28*, 117 – 124.
[37] F. Baletto, R. Ferrando, *Rev. Mod. Phys.* **2005**, *77*, 371 – 423.
[38] F. Baletto, C. Mottet, R. Ferrando, *Phys. Rev. Lett.* **2000**, *84*, 5544 – 5547.

